Title	$\bar{K}$-nuclear bound state at J-PARC
Author(s)	Sakuma Fuminori, Hashimoto Tadashi, Tanida Kiyoshi, 66 of others
Citation	JPS Conference Proceedings, 32, p.010088_1-010088_8
Text Version	Published Journal Article
URL	https://jopss.jaea.go.jp/search/servlet/search?5072446
DOI	https://doi.org/10.7566/JPSCP.32.010088
Right	This article is published by the Physical Society of Japan under the terms of the Creative Commons Attribution 4.0 License. Any further distribution of this work must maintain attribution to the author(s) and the title of the article, journal citation, and DOI.

Proc. 13th Int. Conf. on Nucleus-Nucleus Collisions
JPS Conf. Proc. **32**, 010088 (2020)
https://doi.org/10.7566/JPSCP.32.010088

$\bar{K}$-Nuclear Bound State at J-PARC

Fuminori Sakuma[1], Shuhei Ajimura[2], Hidemitsu Asano[1], George Beer[3], Carolina Berucci[4], Hyoungchan Bhang[5], Mario Bragadireanu[6], Paul Buehler[4], Luigi Busso[7,8], Michael Cargnelli[4], Seonho Choi[5], Catalina Curceanu[9], Shun Enomoto[10], Hiroyuki Fujioka[11], Yuya Fujiwara[12], Tomokazu Fukuda[13], Carlo Guaraldo[9], Tadashi Hashimoto[14], Ryugo S. Hayano[12], Toshihiko Hiraiwa[2], Masami Iio[10], Mihai Iliescu[9], Kentaro Inoue[2], Yosuke Ishiguro[15], Takashi Ishikawa[12], Shigeru Ishimoto[10], Kenta Itahashi[1], Masahiko Iwasaki[1,11], Koki Kanno[12], Kazuma Kato[15], Yuko Kato[1], Shingo Kawasaki[2], Paul Kienle[16]*, Hiroshi Kou[11], Yue Ma[1], Johann Marton[4], Yasuyuki Matsuda[12], Yutaka Mizoi[13], Ombretta Morra[7], Tomofumi Nagae[15], Hiroyuki Noumi[2], Hiroaki Ohnishi[17], Shinji Okada[1], Haruhiko Outa[1], Kristian Piscicchia[18,9], Yuta Sada[2], Atsushi Sakaguchi[2], Masaharu Sato[10], Alessandro Scordo[9], Michiko Sekimoto[10], Hexi Shi[9], Kotaro Shirotori[2], Diana Sirghi[9,6], Florin Sirghi[9,6], Ken Suzuki[4], Shoji Suzuki[10], Takatoshi Suzuki[12], Kiyoshi Tanida[14], Hideyuki Tatsuno[19], Makoto Tokuda[11], Dai Tomono[2], Akihisa Toyoda[10], Kyo Tsukada[17], Oton Vázquez Doce[9,16], Eberhard Widmann[4], Takumi Yamaga[1], Toshimitsu Yamazaki[12,1], Qi Zhang[1], and Johannes Zmeskal[4]
(J-PARC E15 Collaboration)

[1] *RIKEN, Wako, 351-0198, Japan*
[2] *Osaka University, Osaka, 567-0047, Japan*
[3] *University of Victoria, Victoria BC V8W 3P6, Canada*
[4] *Stefan-Meyer-Institut für subatomare Physik, A-1090 Vienna, Austria*
[5] *Seoul National University, Seoul, 151-742, South Korea*
[6] *National Institute of Physics and Nuclear Engineering - IFIN HH, Bucharest - Magurele, Romania*
[7] *INFN Sezione di Torino, 10125 Torino, Italy*
[8] *Universita' di Torino, Torino, Italy*
[9] *Laboratori Nazionali di Frascati dell' INFN, I-00044 Frascati, Italy*
[10] *High Energy Accelerator Research Organization (KEK), Tsukuba, 305-0801, Japan*
[11] *Tokyo Institute of Technology, Tokyo, 152-8551, Japan*
[12] *The University of Tokyo, Tokyo, 113-0033, Japan*
[13] *Osaka Electro-Communication University, Osaka, 572-8530, Japan*
[14] *Japan Atomic Energy Agency, Ibaraki 319-1195, Japan*
[15] *Kyoto University, Kyoto, 606-8502, Japan*
[16] *Technische Universität München, D-85748, Garching, Germany*
[17] *Tohoku University, Sendai, 982-0826, Japan*
[18] *CENTRO FERMI - Museo Storico della Fisica e Centro Studi e Ricerche "Enrico Fermi", 00184 Rome, Italy*
[19] *Lund University, Lund, 221 00, Sweden*

E-mail: sakuma@ribf.riken.jp

(Received July 19, 2019)

$\bar{K}$-nuclear bound states have been widely discussed as a consequence of the strongly attractive $\bar{K}N$ interaction in $I = 0$ channels. Especially, the simplest $\bar{K}$-nuclear bound state of $\bar{K}NN$ (denoted as "$K^- pp$") has attracted the strong interest both of theoretical and experimental studies. We observed a bound state below the $K^- + p + p$ mass threshold with in-flight K^- induced reactions on ^{3}He target, which can be interpreted as the "$K^- pp$" bound state. The possible existence of the "$K^- pp$" state is discussed from both aspects of production and decay: "$K^- pp$" and $\Lambda(1405)p$ productions, and non-mesonic Λp and mesonic $(\pi\Sigma)^0 p$ decays, respectively.

KEYWORDS: $\bar{K}$-nuclear bound states, $\bar{K}NN$, $\Lambda(1405)$, $\bar{K}N$ interaction

1. Introduction

The $\bar{K}N$ interaction is one of the most important probes to understand meson-baryon interactions in low energy quantum chromodynamics (QCD). From extensive measurements of anti-kaonic hydrogen atom [1–3] and low-energy $\bar{K}N$ scattering [4], the strongly attractive $\bar{K}N$ interaction has been revealed in $I = 0$ channel. The strong attraction in $\bar{K}N$ system leads to the possible existence of deeply-bound kaonic nuclear states, which has been widely discussed today [5–21]. The investigation of those exotic states will provide unique information of the $\bar{K}N$ interaction below the threshold, which can not be accessed by the conventional methods. In addition, the great interest of those exotic states is that they might form high-density nuclear matter where the chiral symmetry is expected to be restored. Thus the investigation of the $\bar{K}$ nuclear-states will give us the new insights on not only meson-baryon interactions in low-energy QCD but also the change of the interaction in nuclear media.

Among the kaonic nuclear states, the $\bar{K}NN$ system (symbolically denoted as "K^-pp") is of special interest because it is the lightest predicted $S = -1$ $\bar{K}$ nucleus; this state is expected to be a $[\bar{K} \otimes NN_{I=0,S=0}]_{I=1/2}$ with $J^P = 0^-$. Many theoretical works predicted the existence of the bound state based on a few-body calculation using the $\bar{K}NN - \pi\Sigma N - \pi\Lambda N$ coupled formalism. However, the properties of the bound state, such as the binding energy (B.E.) and the decay width (Γ), strongly depend on the $\bar{K}N$ interaction models. With the energy-independent models (phenomenological models), the binding energy has been predicted to be $\sim 40 - 90$ MeV [6–13], whereas, it becomes $\sim 10 - 30$ MeV in energy-dependent cases (chiral unitary models) [13–19]. In the framework of the chiral model, a double pole structure of the $\bar{K}NN$ is also proposed in relation to $\Lambda(1405)$ [21]. As for the decay width, the predicted values widely spread over $\sim 30 - 110$ MeV. Such divergence is attributed mainly to difference in the $\bar{K}N$ potential below the $\bar{K}N$ mass threshold, which should be experimentally determined by precise measurements of the $\Lambda(1405)$ and of the kaonic nuclear states.

Experimentally, there are several reports on observation of a "K^-pp" candidate with the binding energy of around 100 MeV, in experiments which measured non-mesonic decay branches of Λp and/or $\Sigma^0 p$ in different reactions. The FINUDA experiment measured back-to-back Λp pairs in the stopped K^- reactions on light nuclear targets [22], and the DISTO collaboration analyzed $pp \to \Lambda p K^+$ channel at the proton energy of 2.85 GeV [23]. The obtained spectra, however, can be understood also without the inclusion of a bound state; the AMADEUS collaboration reported that the spectra in the stopped K^- reactions can be well described by K^- multi-nucleon absorption processes with no need of the "K^-pp" component [24, 25], and $K^+\Lambda p$ final state in $p + p$ collision can be explained with resonant and non-resonant intermediate states decaying into $K^+\Lambda$ pair by the HADES collaboration [26]. The J-PARC E27 experiment also reported a bump structure around 100 MeV/c^2 in the $d(\pi^+, K^+)\Lambda p/\Sigma^0 p$ reactions at 1.69 GeV/c [27], but on the other hand the LEPS collaboration reported only upper limits on the cross section for the "K^-pp" bound state in γ induced reactions [28].

Thus, the experimental situation of the "K^-pp" bound state search was also controversial. To clarify whether or not the "K^-pp" bound state exists, a key of the experimental search is to employ a simple reaction and to measure it exclusively. The simple reaction, such as in-flight $\bar{K}$ induced reactions with light target nuclei, would make the "K^-pp" production mechanism clear. The exclusive measurement is crucial to distinguish a small and broad signal from largely and widely distributed

*deceased

quasi-free backgrounds.

2. J-PARC E15 Experiment

To overcome difficulties revealed in the previous experiments, we performed an experiment with K^-+ ^{3}He reactions at 1.0 GeV/c. In the reactions, the "K^-pp" would be produced via the (K^-, n) reaction because a recoiled virtual kaon ('$\bar{K}$') generated by $K^-N \to$ '$\bar{K}$' n processes can be directly induced into the residual two nucleons within the strong interaction range. The momentum of the '$\bar{K}$' is described as the momentum difference of the incident kaon and the outgoing neutron, $q = |\boldsymbol{p}_{K^-}^{lab} - \boldsymbol{n}_n^{lab}|$. When the back scattered '$\bar{K}$' is realized, the q is as small as $\sim$ 200 MeV/c, which makes the "K^-pp" formation probability large. In addition, the "K^-pp" signal such as an expected Λp decay can be kinematically discriminated from considerable backgrounds attributed to multi-nucleon absorption processes and hyperon decays with the exclusive measurement of the Λpn final state.

The experiment was performed at the K1.8BR beam line of the hadron experimental hall at J-PARC [29] (J-PARC E15). The spectrometer consists of a high-precision beam-line, liquid H_2/D_2- and ^{3}He/^{4}He-target systems, a cylindrical detector system (CDS), and a neutron time-of-flight counter array (NC) located ∼15 m downstream from the target position. Decay particles from the target are detected by the CDS which consists of a solenoid magnet, a cylindrical wire drift chamber (CDC), and a cylindrical detector hodoscope (CDH). The CDC contains 15 layers of anode wires, and the CDH consists of 36 modules of scintillators whose thickness is 30 mm mounted on the inner wall of the solenoid magnet. Tracking information of charged particles is obtained from the CDC which operates in a solenoidal magnetic field of 0.7 T, and particle identification is performed using time of flight (TOF) together with a beam-line trigger counter. A detailed description of the spectrometer can be found in Ref. [30].

The first physics run of the E15 experiment was carried out in 2013 with 5.3×10^9 incident kaons on the ^{3}He target. In the semi-inclusive ^{3}He$(K^-, n)X$ spectrum at $\theta_n^{lab} = 0°$, the global spectrum in the unbound region is well reproduced by elementary reactions, whereas a definitive excess of the yield is observed in the bound region [31]. The excess reaching to $\sim$ 100 MeV below the K^- + p + p mass threshold cannot be explained by any simulation result with the elementary reactions, thus the component will be attributed not only to the attractive $\bar{K}N$ interaction but also to the two-nucleon absorption process such as $\bar{K} + NN \to Y^*N$/"K^-pp". To examine the origin of the sub-threshold structure, we conducted the exclusive ^{3}He$(K^-, \Lambda p)n$ analysis which can discriminate huge backgrounds observed in the semi-inclusive ^{3}He$(K^-, n)X$. With the Λpn final state events, we found a peak structure below the mass threshold in the Λp invariant mass spectrum [32]. We also found that the structure is concentrated in the the low momentum-transfer region of the (K^-, n) reactions as expected. This Λp spectrum is theoretically interpreted as the $\bar{K}NN$ bound system based on the chiral unitary approach [33]; the experimental spectrum is well reproduced by the assumption of the $\bar{K}NN$ bound system. To confirm the peak structure observed in the Λp spectrum, the second physics run was carried out in 2015 with 32.5×10^9 incident kaons on the ^{3}He target. By focusing data taking of the Λpn events, we successfully accumulated $\sim$ 30 times more data on the Λpn final state.

3. Λpn Final State

To reconstruct the Λpn final state, two protons and one negative pion was requested in the CDS, and a missing neutron was identified by missing mass of ^{3}He$(K^-, pp\pi^-)n$. The $p\pi^-$ pair associated with the Λ decay in the $pp\pi^-$ event was selected with a log-likelihood method taking into account distance of closest approach of measured tracks and kinematical fit with energy-momentum conservation of the reaction. The reaction of K^-+ ^{3}He $\to$ "K^-pp" $+n \to \Lambda + p + n$ can be uniquely described by the two parameters of the Λp invariant mass $IM(\Lambda p)$ and the momentum transfer q. Figure 1

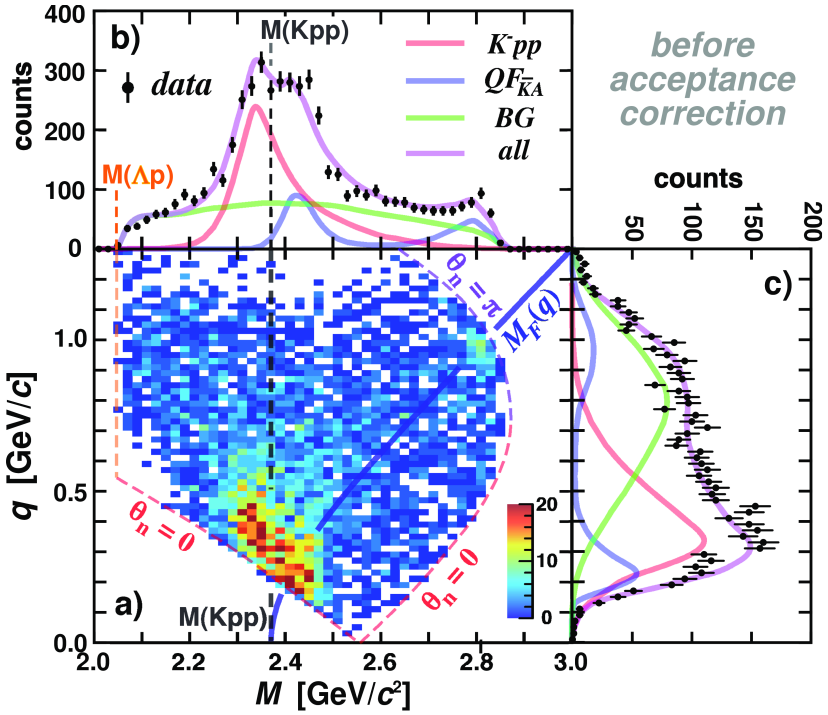

Fig. 1. (a) Event distribution on the M (= $IM(\Lambda p)$) and the momentum transfer q for the Λpn final state. The projected histograms onto (b) the M axis and (c) q axis. The fitting results with the simple model are also plotted as colored curves. The Figure is taken from Ref. [34].

shows the event distribution of q and $IM(\Lambda p)$. As shown in Fig. 1(a), a strong event concentration near the mass threshold of $K^- + p + p$ at the lower q region can be seen as previously observed in Ref. [32].

The high statistics data in the second physics run makes us possible to examine the structure near the K^-+p+p mass threshold in detail. The structure near the threshold is found to be composed of two structures, which cannot be represented as a single Breit-Wigner function as assumed in the previous analysis. The centroid of a structure just below the mass threshold does not depend on q within the statistical uncertainty, whose yield decreases to $q \sim 650$ MeV/c. This behavior is an strong evidence of an existence of a bound state. On the other hand, the distribution centroid above the mass threshold depends on q, *i.e.* the centroid shift to heavier mass for the larger q. The natural interpretation of the structure above the threshold is non-resonant absorption of the backward quasi-free '$\bar{K}$' ($\theta_n^{CM} = 0$) by the NN spectator, where the '$\bar{K}$' propagates as an on-shell particle. The Λp final state is generated by the '$\bar{K}$' $+NN \rightarrow \Lambda p$ conversion due to the final state interaction. Indeed, another event concentration can be seen around $IM(\Lambda p) \sim 2.8$ GeV/c^2, which is originated from the forward quasi-free '$\bar{K}$' ($\theta_n^{CM} = \pi$) where the neutron remains as a spectator.

We performed the simplest model fit to reproduce the event distribution with the bound state, the quasi-free process, and a broad background distributed over the Λpn phase space. The data was fitted by using the maximum likelihood method in the 2D space of $q - IM(\Lambda p)$ shown in Fig. 1(a). The details of the fitting can be found in Ref. [34]. The simple fitting well reproduces the event distribution whose result is shown in Fig 1(b) and (c) as colored curves. At the lower q region below 0.35 GeV/c, however, the signal from the bound state and the quasi-free contribution are hardly separated because the interference between the bound state formation and the quasi-free process is expected near the kinematical boundary. To show the bound state clearly, we plot the Λp invariant

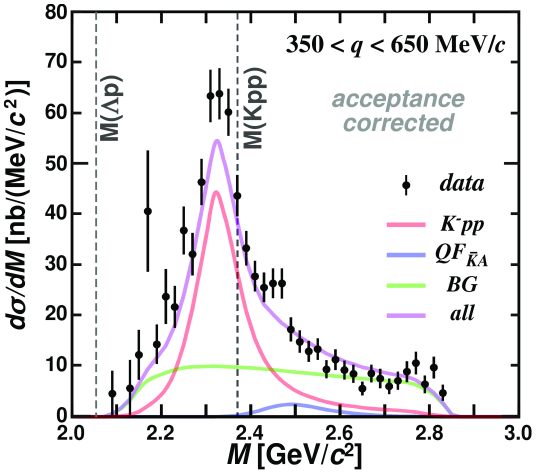

Fig. 2. Efficiency and acceptance corrected Λp invariant mass in the region of $0.35 < q < 0.65$ MeV [34].

mass spectrum corrected by the detector acceptance and the experimental efficiency in the momentum transfer window of $350 < q < 650$ MeV/c as Fig. 2. In the figure, the yields of other processes are largely suppressed in contrast to the bound state, and the quasi-free distribution is also clearly separated from the peak of the bound state.

The simplest fit to the observed peak structure give us a Breit-Wigner pole position at $M = 2324 \pm 3(stat.)^{+6}_{-3}(syst.)$ MeV/c^2 (*i.e.* a binding energy $B = 47 \pm 3(stat.)^{+6}_{-3}(syst.)$ MeV/c^2) with a width $\Gamma = 115 \pm 7(stat.)^{+10}_{-20}(syst.)$ MeV/c^2, and the S-wave Gaussian form factor parameter $Q = 381 \pm 14(stat.)^{+57}_{0}(syst.)$ MeV/c^2. Thus the peak structure is well below the $K^- + p + p$ mass threshold, and significantly above the $\Lambda + p$ mass threshold. In addition, the structure cannot be reproduced any background process such as $Y^{(*)}$ production in two nucleon absorption processes followed by Λp conversion: $K^-\,{}^3\mathrm{He} \to Y^{(*)}NN_R \to \Lambda pn$, where N_R denotes a residual nucleon. Therefore, the natural and simplest interpretation of the peak structure is the "$K^- pp$" bound state.

The obtained binding energy of ~ 50 MeV is deeper than chiral SU(3) motivated calculations [13–19], while the almost consistent with the phenomenological based calculations [6–13]. The width of ~ 100 MeV is rather wide compared to theoretical calculations which take into account only mesonic decay channels such as $\pi\Sigma N$ decay branches. Thus the observed large width indicates that contribution form non-mesonic decays cannot be ignored in the theoretical calculations. The observed values of the large form factor ~ 400 MeV/c and the large binding energy ~ 50 MeV imply the formation of a compact system. To deduce its size quantitatively, however, theoretically sophisticated analysis is required because the form factor parameter is obtained from the simple momentum transfer analysis based on PWIA in the current analysis.

4. Λ(1405)*pn* Final State

As described above, we found the "$K^- pp$" bound state in Λpn final state. Then a question arises whether or not the "$K^- p$" bound state is also produced in the same K^- + ^{3}He reaction. The $\Lambda(1405)$ state, which decays into $\pi\Sigma$, is theoretically considered as a quasi-bound state of $\bar{K}N$ in $I = 0$ as supported by a lattice QCD calculation [35]. Thus we should observe not only the "$K^- pp$" bound state but also the $\Lambda(1405)$ state in the same K^- + ^{3}He reactions. Indeed, the production mechanism of the $\bar{K}NN$ system is theoretically understood with a $\Lambda(1405) + N \to \bar{K}NN$ doorway process. Furthermore, from a theoretical point of view, the $\bar{K}NN$ is a resonant state in the $\bar{K}NN - \pi\Sigma N - \pi\Lambda N$ coupled-channel system, and the mesonic $\pi\Sigma N$ decays are expected to be dominant compared to the non-

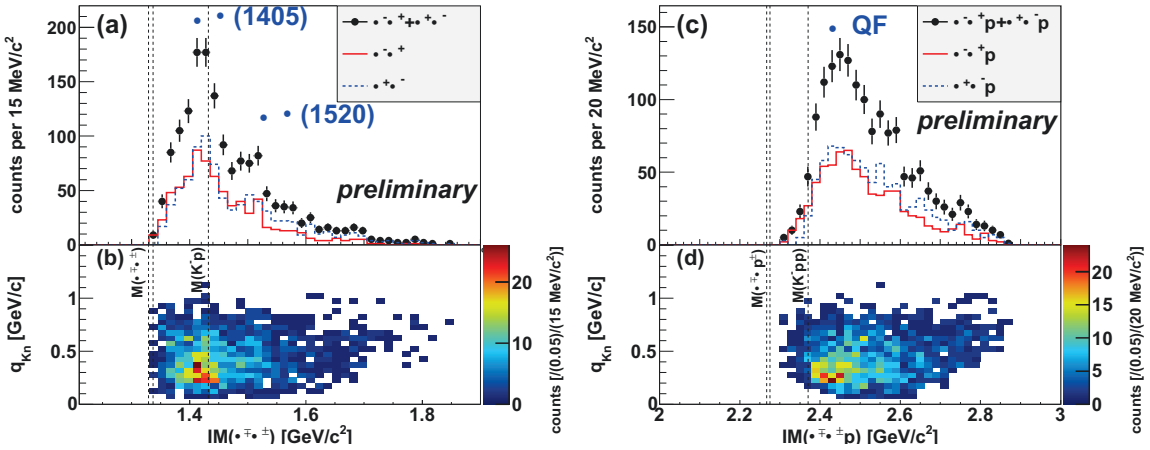

Fig. 3. (a) Invariant mass of $\pi^{\pm}\Sigma^{\mp}$ and (b) event distribution on the momentum transfer q and the $IM(\pi^{\pm}\Sigma^{\mp})$ for the $\pi^{\pm}\Sigma^{\mp}pn$ final state. (c) $IM(\pi^{\pm}\Sigma^{\mp}p)$ and (d) q versus $IM(\pi^{\pm}\Sigma^{\mp}p)$.

mesonic YN decays [36]. This is because the kaon absorption probability of the $(Y_K)_{I=0} + N \to \pi\Sigma N$ reactions are significant, where $(Y_K)_{I=0}$ denotes an isobar of $\bar{K}N$ states with $I = 0$. Measurements of the mesonic $\pi\Sigma N$ channels originated from the $\bar{K}NN$ decay and the $\Lambda(1405)p$ production are therefore indispensable to obtain further information on the kaonic nuclear bound systems.

For this purpose, events from K^-+ ^{3}He $\to$ $\pi^{\pm}\Sigma^{\mp}pn$ reactions were selected in the analysis. $\pi^{\pm}\Sigma^{\mp}p \to \pi^+\pi^-np$ were detected with the CDS, where *the neutron from the* $\Sigma^{\pm}$ *decays* was obtained using the CDH by requiring no charged track in front of a CDH hit and no hits in both neighboring side of the CDH segment. *The neutron* was identified with analysis cuts of $1/\beta$ more than 1.372 (corresponding to less than 1 GeV/c neutron) and energy loss (dE) more than 2 MeV electron equivalent (MeVee). The other neutron in the reaction was identified with the missing-mass method of ^{3}He$(K^-, \pi^+\pi^-np)X$ with $X = n$.

After the $\pi^+\pi^-pn$ reconstruction with the CDS, a kinematic fit was applied whether the event is consistent with the ^{3}He$(K^-, \pi^{\pm}\Sigma^{\mp}p)n$ reaction kinematics. In the fit, the momenta of measured tracks were recalculated with the assumption of physical constraints of 4-momentum conservation and invariant mass of the $\Sigma^{\pm} \to \pi^{\pm}n$ decays. The event selection of the $\pi^{\pm}\Sigma^{\mp}pn$ final state was performed using the chi-square test of the event hypothesis. The fit was applied twice for each event with the two hypotheses of the $\pi^+\Sigma^-pn$ and $\pi^-\Sigma^+pn$ final states. The $\pi^+\Sigma^-pn$ state should give a larger χ^2 probability (p-value) for events with the $\pi^+\Sigma^-pn$ hypothesis than that with the $\pi^-\Sigma^+pn$, and vice versa. We selected the final events fulfilling the hypothesis with p-value more than 0.01.

Figures 3(a) and (b) show the invariant mass of $\pi^{\pm}\Sigma^{\mp}$ and the event distributions as a function of q_{Kn}, respectively. A $\Lambda(1405)$ peak clearly exists below the $K^- + p$ mass threshold, whose events concentrate in the low momentum transfer region. Figures 3(c) and (d) show the invariant mass of $\pi^{\pm}\Sigma^{\mp}p$ and its event distributions, respectively. One can see that a structure above the $K^- + p + p$ mass threshold is also concentrated in the low momentum transfer region, which locates on the mass position of the $K^-N \to \bar{K}n$ quasi-free processes with forward neutron emission [$IM(\pi^{\pm}\Sigma^{\mp}p) \sim 2.4$ GeV/c^2]. The results mean that the $K^-N \to$ '$\bar{K}$'n quasi-free processes followed by the '$\bar{K}$'$+NN \to \Lambda(1405)p$ reaction is dominant. We already found that the "K^-pp" bound state is produced via lower momentum transfer of the $K^-N \to$ '$\bar{K}$'n quasi-free processes followed by the two-nucleon absorption of '$\bar{K}$'$+NN \to$ "K^-pp", therefore, the production mechanism of the "K^-pp" and $\Lambda(1405)p$ states will be quite similar except for the final state.

However, in contrast to the Λpn final state, one can see that those $\Lambda(1405)pn$ events mainly

distribute above the $K^- + p + p$ mass threshold in the $\pi^\pm\Sigma^\mp p$ invariant-mass spectrum as shown in 3(c). Focusing on the region below the $K^- + p + p$ mass threshold, no clear structure was found below the threshold where we observed the "K^-pp" peak in the Λp invariant-mass spectrum. This will be due to small $\pi\Sigma N$-decay branches of the "K^-pp" bound state, which are theoretically expected to be dominant decay channels as discussed in Ref. [36]. This discrepancy can be naively interpreted using the decay phase-space volume of the "K^-pp". The $\pi\Sigma N$-decay phase space below the $K^- + p + p$ mass threshold is kinematically limited, thus the decay branches into non-mesonic YN channels can be widely opened when the "K^-pp" bound state is formed. This interpretation is consistent with our observation of the "K^-pp" in the Λp channel; the obtained width of $\sim$ 100 MeV is larger than theoretical expectations based on the mesonic $\pi\Sigma N$ decays. In addition, this $\pi\Sigma N$ phase-space limitation will distort the spectral shape of the "K^-pp" toward the $K^- + p + p$ mass threshold, in case of the "K^-pp" binding energy of $\sim$ 50 MeV we observed. Thus, in the $\pi\Sigma N$ channel, it will be possible that the "K^-pp" is observed as a shoulder below the quasi-free tail, not a peak below the $K^- + p + p$ mass threshold.

To compare the cross section between the Λpn final state and $\pi^\pm\Sigma^\mp pn(\Lambda(1405)pn)$, the efficiency correction was performed event-by-event by considering the event kinematics of the $\pi\Sigma pn$ final state. The efficiency, including the detector acceptance and event-reconstruction efficiency, was evaluated with a full Monte-Carlo simulation using the $\pi^\pm\Sigma^\mp pn$ phase space. After subtraction of $\pi^+\pi^- pnY$ contaminations in the $\pi^\pm\Sigma^\mp pn$ final state, where Y cannot be detected by the CDS and those widely spreaded event distribution gets in the region of interest of $\pi^\pm\Sigma^\mp pn$, we evaluated the cross section of the $\Lambda(1405)pn$ final state to be $\sim$ 100 μb. The evaluation was performed by fitting the spectrum with $\Sigma(1385)$ whose yield was estimated from $\Sigma(1385)^\pm$ channel, $\Lambda(1405)$, $\Lambda(1520)$, and a non-resonant $\pi^\pm\Sigma^\mp$ background. For the $\Lambda(1405)$, we simply adopted a Flatté parametrization [37]. Details of the analysis will be given in a forthcoming publication.

The obtained $\Lambda(1405)p$ cross section is $\sim$ 10 times larger than that of the "K^-pp" bound state evaluated to be $\sigma^{tot}_{K^-pp} \cdot Br_{\Lambda p} = 11.8 \pm 0.3(syst.)^{+0.6}_{-1.0}(syst.)$ μb [34]. It can be understood by considering the scattered-kaon energy of the first-step $K^-N \to$ '$\bar{K}$'n process in the laboratory frame (E^{lab}_K) as follows. When the scattered-kaon energy is above its intrinsic mass m_K ($E^{lab}_K > m_K$), the '$\bar{K}$'$+NN \to \Lambda(1405)p$ reaction is dominant. The energy-momentum mismatch has to be transferred to the proton, *i.e.,* the "K^-p" bound state as the $\Lambda(1405)$ state is formed above the $K^- + p + p$ mass threshold. On the other hand, when the kaon energy is below the intrinsic mass ($E^{lab}_K < m_K$), the "K^-pp" bound state is formed via the '$\bar{K}$'$+NN \to$ "K^-pp" reaction. The "K^-pp" is produced via '$\bar{K}$' capture by two residual nucleons under the energy-momentum match condition below the mass threshold.

5. Conclusion and Prospect

An experimental search for the $\bar{K}NN$ bound state was performed at J-PARC by using the in-flight K^- + ^{3}He reactions at 1 GeV/c. We observed a significant peak structure well below the $K^- + p + p$ mass threshold in the Λp invariant-mass spectrum of the Λpn final state, whose natural and simple interpretation is the "K^-pp" bound state. We also successfully measured $\Lambda(1405)pn$ final state in the K^- + ^{3}He reactions by reconstructing $\pi^\mp\Sigma^\pm pn$ events, which distributes above the mass threshold in the $\pi^\pm\Sigma^\mp p$ invariant-mass spectrum. The production cross section of the $\Lambda(1405)p$ was $\sim$10 times larger than that of the "K^-pp" bound state observed in the Λp invariant mass, which will provide quite important information on the production mechanism of the "K^-pp" bound state.

To obtain further understanding of the kaonic nuclei, we are planing to perform the systematic study of the kaonic nuclear bound states in light nuclei, from the "$\bar{K}N$" to "$\bar{K}NNNN$", via the in-flight (K^-, N) reactions with a new 4π spectrometer. In the new experiment, we measure nuclear mass number dependence of the kaonic-nuclei properties and determine decay branches. Such systematic study provides quite unique information about the $\bar{K}N$ interaction in the region below the mass threshold,

which is of importance to gain a further understanding of the low-energy QCD.

References

[1] M. Iwasaki *et al.*, Phys. Rev. Lett. **78**, 3067 (1997).
[2] G. Beer *et al.*, Phys. Rev. Lett. **94**, 212302 (2005).
[3] M. Bazzi *et al.*, Phys. Lett. **B704**, 113 (2011).
[4] A. D. Martin, Nucl. Phys. **B179**, 33 (1981).
[5] Y. Akaishi and T. Yamazaki, Phys. Rev. **C65**, 044005 (2002).
[6] T. Yamazaki and Y. Akaishi, Phys. Lett. **B535**, 70 (2002).
[7] N. V. Shevchenko, A. Gal, and J. Mares, Phys. Rev. Lett. **98**, 082301 (2007).
[8] N. V. Shevchenko, A. Gal, J. Mares, and J. Révai, Phys. Rev. **C76**, 044004 (2007).
[9] Y. Ikeda and T. Sato, Phys. Rev. **C76**, 035203 (2007).
[10] Y. Ikeda and T. Sato, Phys. Rev. **C79**, 035201 (2009).
[11] S. Wycech and A. M. Green, Phys. Rev. **C79**, 014001 (2009).
[12] A. Dote, T. Inoue, and T. Myo, Phys. Rev. **C95**, 062201 (2017).
[13] J. Révai and N. V. Shevchenko, Phys. Rev. **C90**, 034004 (2014).
[14] N. Barnea, A. Gal, and E. Z. Liverts, Phys. Lett. **B712**, 132 (2012).
[15] A. Dote, T. Hyodo, and W. Weise, Nucl. Phys. **A804**, 197 (2008).
[16] A. Dote, T. Hyodo, and W. Weise, Phys. Rev. **C79**, 014003 (2009).
[17] Y. Ikeda, H. Kamano, and T. Sato, Prog. Theor. Phys. **124**, 533 (2010).
[18] M. Bayar and E. Oset, Phys. Rev. **C88**, 044003 (2013).
[19] A. Dote, T. Inoue, and T. Myo, Phys. Lett. **B784**, 405 (2018).
[20] S. Maeda, Y. Akaishi, and T. Yamazaki, Proc. Jpn. Acad. **B89**, 418 (2013).
[21] A. Dote, T. Inoue, and T. Myo, Prog. Theor. Exp. Phys. **2015**, 043D02 (2015).
[22] M. Agnello *et al.*, Phys. Rev. Lett. **94**, 212303 (2005).
[23] T. Yamazaki *et al.*, Phys. Rev. Lett. **104**, 132502 (2010).
[24] O. Vázquez Doce *et al.*, Phys. Lett. **B758**, 134 (2016).
[25] R. Del Grande *et al.*, Eur. Phys. J. **C79**, 190 (2019).
[26] G. Agakishiev *et al.*, Phys. Lett. **B742**, 242 (2015).
[27] Y. Ichikawa *et al.*, Prog. Theor. Exp. Phys. **2015**, 021D01 (2015).
[28] A. O. Tokiyasu *et al.*, Phys. Lett. **B728**, 616 (2014).
[29] K. Agari *et al.*, Prog. Theor. Exp. Phys. **2012**, 02B009 (2012).
[30] K. Agari *et al.*, Prog. Theor. Exp. Phys. **2012**, 02B011 (2012).
[31] T. Hashimoto *et al.*, Prog. Theor. Exp. Phys. **2015**, 061D01 (2015).
[32] Y. Sada *et al.*, Prog. Theor. Exp. Phys. **2016**, 051D01 (2016).
[33] T. Sekihara, E. Oset, and A. Ramos, Prog. Theor. Exp. Phys. **2016**, 123D03 (2016).
[34] S. Ajimura *et al.*, Phys. Lett. **B789**, 620 (2019).
[35] J. M. M. Hall *et al.*, Phys. Rev. Lett. **114**, 132002 (2015).
[36] S. Ohnishi, Y. Ikeda, H. Kamano, and T. Sato, Phys. Rev. **C88**, 025204 (2013).
[37] S. M. Flatté, Phys. Lett. **63B**, 224 (1976).